International Journal of
Electrical Machine Analysis and Design

Volume 3, Issue 1, 2025
January–June
DOI (Journal): 10.37591/IJEMAD

https://journals.stmjournals.com/ijemad

Research IJEMAD

TZSBLC With Optimized PI Controller Design for Grid-Tied PV-Based Electric Vehicle

Aran Glenn J.*

Abstract

Around the world, about 18% premature births and 3.7 million losses of lives occur due to air pollution and 29% of it is contributed by the internal combustion engine (ICE) based vehicles, which consume fossil fuels for their functioning. Moreover, the increased demand for fossil fuels, as well as the growth in concerns regarding the environmentally friendly and zero-emission transportation, led to the introduction of electric vehicles (EVs). The increased growth in EV sales starting from 3.1 million (2020) to 14 million (2025), resulted in the necessity for better EV charging facilities. The increased cost and short life span of batteries leads to high EV reliability issues, restricted driving range and charging time. Besides, the vast penetration of EVs creates high strain on the grid, at the time of charging, as EV involves consumption of huge energy within a short duration of time. These concerns corresponding to EVs are eradicated with the integration of renewable energy sources (RES) like solar, wind, tidal, biomass, etc. into the EV infrastructure and it gains increased popularity, as they decrease the grid burdens, greenhouse gas (GHG) emissions and charging costs. A novel trans Z-source Luo converter is used to enhance the photovoltaic (PV) output voltage thereby lessening the number of PV panels used. The proposed converter exhibits the benefits like excellent efficiency, lesser voltage stress and high conversion range. The operation of the proposed converter is regulated with the aid of Lion Grey Wolf optimized proportional integral (LGWO-PI) controller which significantly strengthens the converter operation in terms of settling time, total harmonic distortion (THD) and peak overshoot. The obtained converter output energizes the brushless direct current motor (BLDC) motor of EV after its conversion to AC form by a voltage source inverter (VSI). A conventional PI controller is used for the effective speed control of BLDC motor. At times of power unavailability from PV systems, a VSI fed grid is used to energize the BLDC motor. Overall, the complete charging setup provides a constant power supply for EVs. The presented work is simulated using MATLAB and the output indicates the enhanced functioning of the charging system. Comparisons are carried out with existing converters and control approaches in which the proposed system delivers a reduced THD of 2.1% and an optimal efficiency of 97.6%.

Keywords: Photovoltaic (PV) system, boost converter, Lion Grey Wolf Optimized proportional integral (LGWO-PI) controller, brushless direct current (BLDC) motor, proportional integral (PI) controller, single phase voltage source inverter (VSI), three phase VSI, electric vehicle (EV) charging

***Author for Correspondence**
Aran Glenn J.
E-mail: aranglenn@gmail.com

Visiting Professor, Department of Electrical and Electronics Engineering, Dayananda Sagar College of Engineering (Autonomous), Bengaluru, Karnataka, India

Received Date: March 15, 2025
Accepted Date: March 25, 2025
Published Date: April 07, 2025

Citation: Aran Glenn J. TZSBLC With Optimized PI Controller Design for Grid-Tied PV-Based Electric Vehicle. International Journal of Electrical Machine Analysis and Design. 2025; 3(1): 18–36p.

INTRODUCTION

Solar energy, which is the one among the renewable energy sources (RESs), is an environmentally friendly energy source with reduced installation costs and reduced maintenance. Even though the photovoltaic (PV) system possesses many advantages, it also possesses drawbacks like high voltage fluctuations and reduced DC link voltage maintenance. Since, the output of PV changes with respect to the climatic conditions, it is impossible to attain constant output from the PV system, thereby necessitating DC-DC converters, which enhances the output of the PV system. The PV-fed grid-tied system necessitates DC-DC and DC-AC converters for the power transfer. In order to improve the PV output, many DC-DC converters like boost, buck-boost, Cuk, SEPIC and Zeta, converters are employed and these converters transforms the low voltage output of PV to a higher level. Moreover, due to the fluctuating nature of PV system, it is difficult to obtain constant DC-link voltage, hence appropriate control techniques have to be implemented for improving the performance of the converter, thereby brings reduced THD (total harmonic distortion), reduced peak overshoot issues and less steady state error. The control techniques mostly prefer proportional integral (PI) controller for regulating the DC-link voltage. Moreover, for tuning the control parameters of the PI controller various optimization algorithms are employed. Then, through VSI (voltage source inverter), the DC-link voltage achieved from the PV system is supplied to the grid or the motor of the electric vehicle (EV). The grid synchronization, as well as the speed control in EV motor are performed with the aid of PI controllers. This research involves a novel Trans-Z-source based Luo converter along with optimum PI controller for the PV-fed grid-tied EV system [1–5].

In order to ensure and maintain secure consistent grid operation, this method required to balance electricity production and electric vehicle charging. One of the major issues that needs to be fixed for power system to operate correctly in future is the erratic nature of RES generation. Normally, power control and operational strategy execution under various load operating states do not work well with load oscillation management to balance the grid. The planning of loads usually involves regulating the rate of RES generation, which has been suggested because additional electricity manufacture schedule is essential for functions of current systems. Moreover, EVs have indicated their capacity to assist main grid with sustaining a specific quantity of both demand and give equilibrium, that increase the chances of RES penetration. In reality, this topic was covered in several published research studies. Furthermore, since the energy needs of these cars do not substantially increase the overall load, PV output may encourage the wider adoption of EVs. However, either differently or together, the inclusion of EV source and PV source into the grid requires adequate planning; or else, system consistency can be compromised. A main factor in PV production, in the eyes of power grid operators, involves durable unpredictability. An issue with electric vehicle source is that it may disrupt a demand side as well as result in grid overload, which may lower power quality and grid stability. It is necessary to plan and manage how EV and PV are integrated into the grid; for instance, by using a scheduled load approach, it is possible to improve the penetration of EVs and PVs into grid [6–9].

It is clear that using RES in EV charging systems is advantageous because it (i) reduces load on grid caused by EVs, (ii) fixes voltage control issues with electricity grid, (iii) lowers utilizing , (iv) broadens energy storage by raising renewable production, (v) enhances the efficiency of both vehicle-to-grid and vehicle-to-home strategies, (vi) reduces fuel costs, and (vii) stops CO_2 emissions. Hydropower, biogas, fuel cells, PV energy, and other renewable energy source are good potential sources to charge, power EVs. These methods, when paired with energy storage systems, relevant electrical equipment, and proper connection techniques, meet the needs of EV charging. More RES can be used to fuel EVs and use local power sources, including RES [10–17].

Nowadays, RES, especially PV, Wind Turbine (WT), and biomass energy, are able to increase power generation in the power system. Due to their high energy density, low construction costs, ease of application, and improved power generation efficiency, they are usually used to conveniently charge EVs. Due to the high intensity of solar radiation on Earth's surface and its non-polluting and silent nature, solar energy remains highly exploitable. The stand-alone PV system is typically unreliable because the climate and surrounding environment have an impact on how much electricity it can produce. However, the PV modules stand out for their clear and simple design, compact size, low weight, and consistency during installation and transport. Additionally, the PV system can be easily installed with other power sources, employed in homes or other buildings, and requires less time for construction.

The variation in the output of a PV system can be reduced significantly by a system for energy storage at the charging point. There are many reasons to use PV solar panels to charge EVs.

- PV panels can be deployed in parking areas close to EV parking areas and on rooftops.
- In latest generations, the price of solar PV panel has steadily decreased.
- Because some of the charging power is generated by PV panel, the peak demand for EVs charging at the grid side is decreased.
- Solar energy is more affordable than grid-based systems for charging EVs.
- The power generated by photovoltaic panels is retained by PV charging systems using a battery storage system (BSS), which assists in regulating day and seasonal climate variations that impact solar production.

The charging of EVs from PV panel has potential to make EVs more ecologically and cost effective by reducing the overall charging facility costs, which is essential due to the current power grid structure and the fast development of EVs load where the correction of the primary energy structure of a grid side greatly raises the cost of power grid transition [18–26].

PROPOSED SYSTEM DESCRIPTION

In recent times, the increased exhaustion of fossil fuels and the necessity for curtailment in carbon emission, lead to the introduction of EV concept, which assists in decarbonized energy generation and transportation and this further helps in reducing the global warming issues. In the proposed research, a PV-fed grid-tied EV system is introduced. For improving the output of the PV panel, a novel DC-DC trans-Z source based Luo converter is employed.

Figure 1 illustrates the block diagram representation of the proposed research work. Then, to maintain stable DC-link voltage, a hybrid Lion Grey Wolf Optimization algorithm based closed loop technique is employed. Furthermore, the stable DC-link voltage obtained is transformed into AC supply with the aid of three phase VSI and is then given to the brushless direct current (BLDC) motor of the EV.

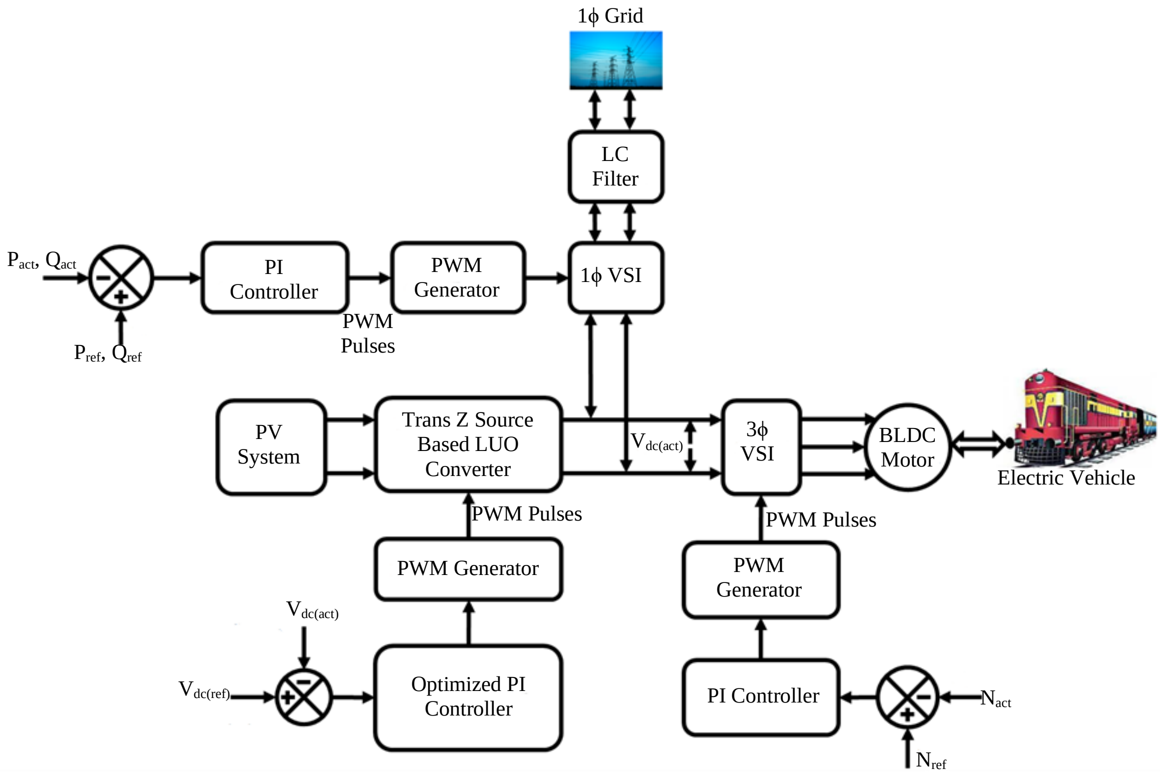

Figure 1. Block diagram illustration of the proposed work.

Then, for regulating the speed of the BLDC motor, a PI controller is employed and then through a PWM (pulse width modulation) generator, the PWM pulses are produced and given to the three phase VSI. Furthermore, the excess energy generated by the PV system is supplied to the single phase grid using single phase VSI. For attaining grid synchronization, a PI controller is employed through which the phase and voltage of the grid and the VSI are bought equal. Using the proposed research better energy management, less THD, better reactive power compensation, reduced losses and efficient speed regulation are attained.

PROPOSED SYSTEM MODELLING

TZSBLC Converter

In a PV system, a solar irradiation is converted into photo-generated current using PV principle. By using TZSBLC, a PV production is increased to its maximum potential. Trans Z-source converter and Luo converter characteristics are combined to hybrid converter known as the TZSBLC as shown in Figure 2. A power switchS_1, four diodes (D_1,D_2, D_3 D_4), 5 capacitors (C_1, C_2, C_3, C_4 C_o), three inductors (L_1, L_2, and L_3), and a load resistor R make a proposed converter, as illustrated in Figure 2. CCM is a converter's mode of operation. Figure 3 depicts a converter's two operational modes.

Mode 1

At this mode of operation, a power switch S 1 stays in ON position. Due to reverse bias, diodes D_1,D_3, and D_4 stop conducting. The diode D_2 is a forward biased in its current state. Through a use of a capacitor C_3 and source voltage V_{PV}, the inductor L_1 begins to store energy. A capacitor C_1 starts to charge as the inductor L_2 releases its stored energy.

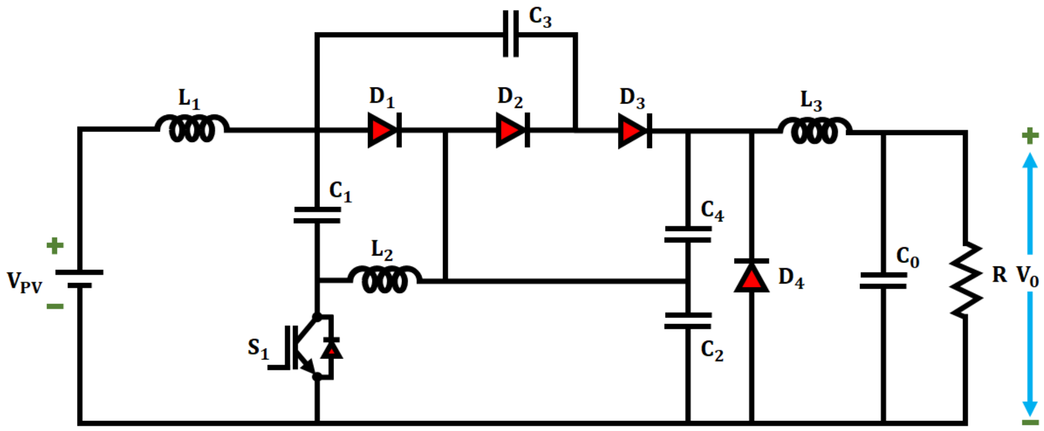

Figure 2. Trans-Z source based Luo converter (TZSBLC) circuit diagram.

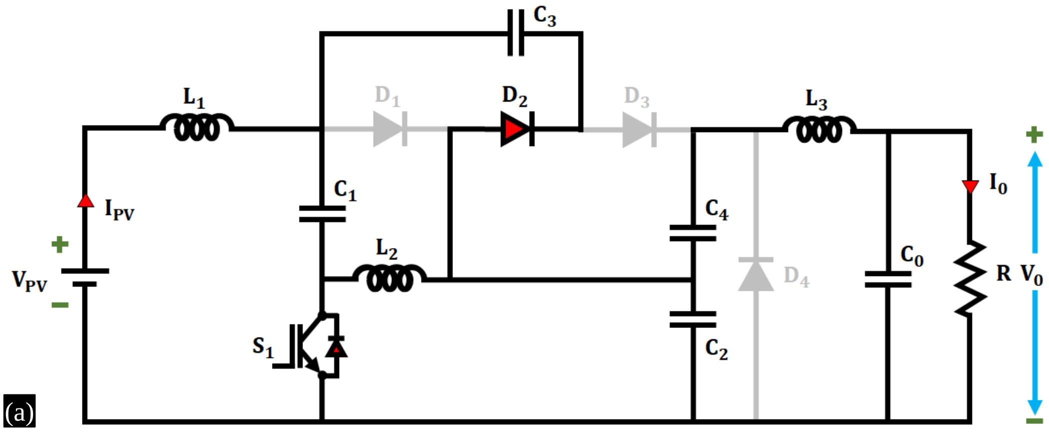

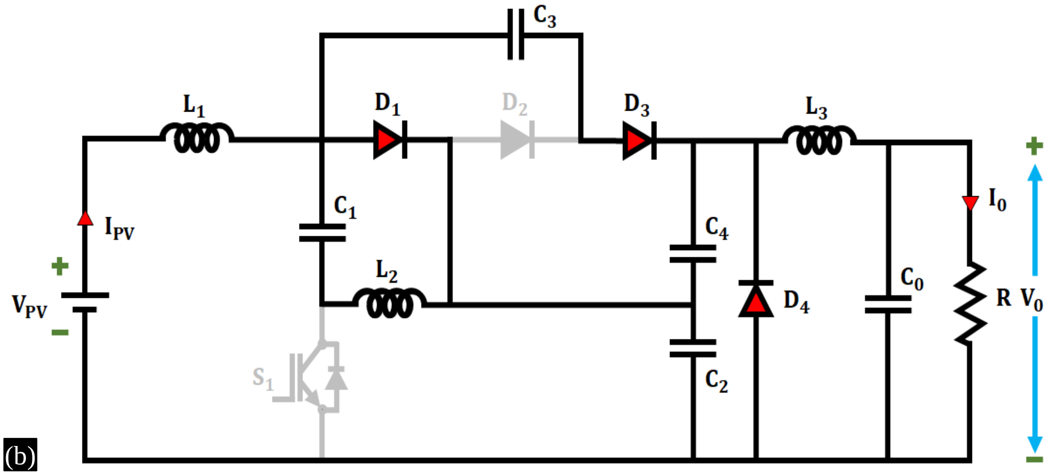

Figure 3. Circuit diagrams of (a) Mode 1 operation and (b) Mode 2 operation.

Mode 2

The power switch S_1 remains in OFF state at a mode of operation. Diodes D_1, D_3 and D_4 are forward biased and begin to conduct. A diode D_2 breaks conducting as it is reverse biased while a load is excited by an input DC source through inductor L_1. The current and voltage waveforms of TZSBLC are shown in Figure 4. The output voltage attained from TZSBLC is,

$$V_O = \left(\frac{2-D}{1-2D}\right) V_{PV} \tag{1}$$

The value of the inductors L_1,L_2, and L_3 are given as,

$$L_1 = \frac{D(1-D)V_{PV}}{\Delta i_{L_1} f_s (1-2D)} \tag{2}$$

$$L_2 = \frac{D(1-D)V_{PV}}{\Delta i_{L_2} f_s (1-2D)} \tag{3}$$

$$L_3 = \frac{DV_{PV}}{\Delta i_{L_3} f_s} \tag{4}$$

The C_1,C_2, C_3 C_4 values are computed as,

$$C_1 = \frac{(1-D)I_{L_2}}{\Delta V_{C_1} f_s} \tag{5}$$

$$C_2 = \frac{(1-D)I_{L_2}}{\Delta V_{C_2} f_s} \tag{6}$$

$$C_3 = \frac{DI_O}{\Delta V_{C_3} f_s (1-D)} \tag{7}$$

$$C_4 = \frac{DI_O}{\Delta V_{C_4} f_s} \tag{8}$$

The value of the output capacitor is,

$$C_o = \frac{DV_{PV}}{8\Delta V_O L_3 {f_s}^2} \tag{9}$$

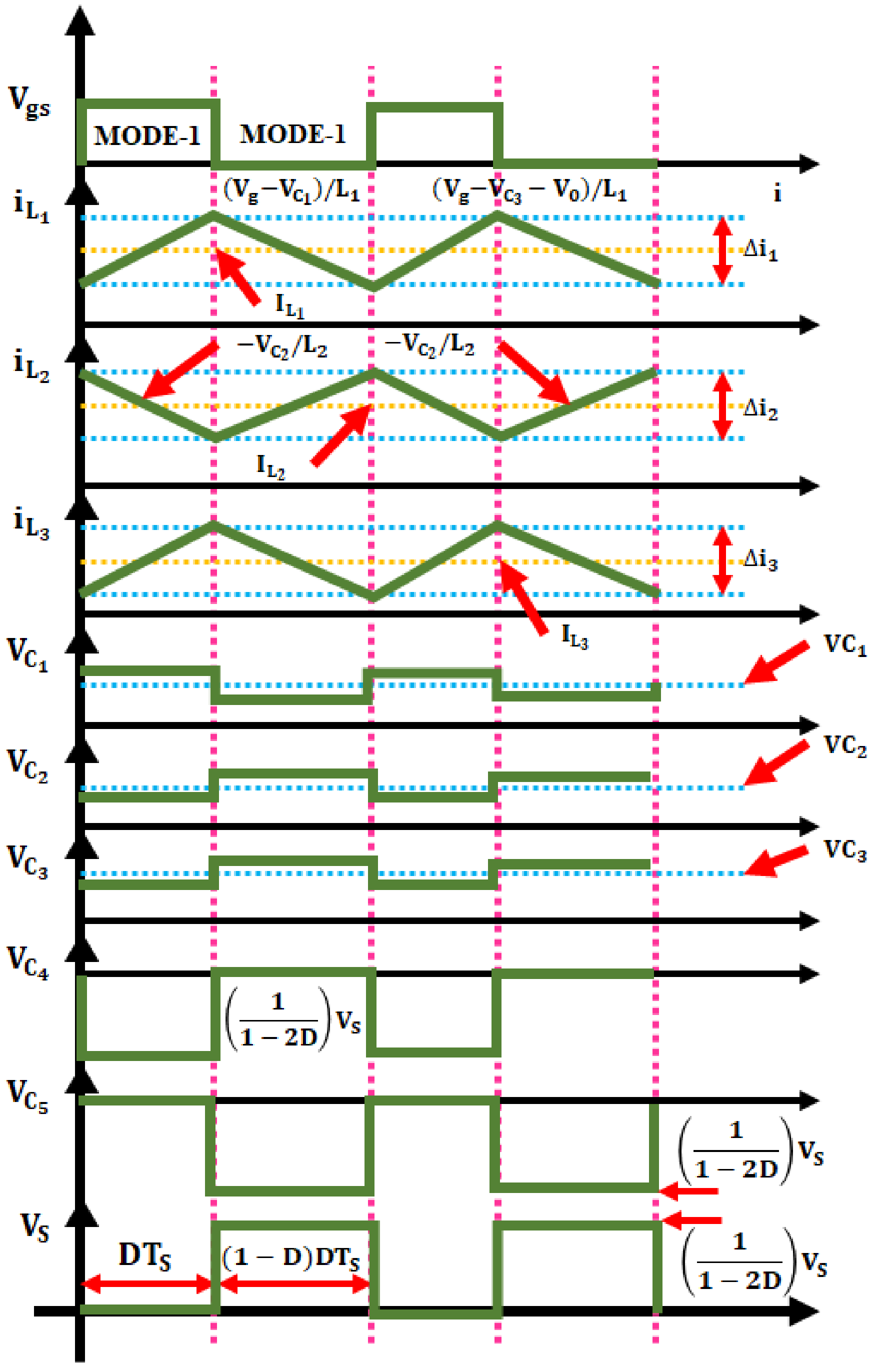

Figure 4. Current and voltage waveforms of trans-Z source based Luo converter (TZSBLC).

The unbalanced DC output voltage gained from a converter is optimized provide stable with the assistance of optimized PI controller.

RESULTS AND DISCUSSION

The proposed work is simulated using MATLAB Simulink and the corresponding result obtained are as follows. The specifications of the converter are mentioned in Table 1.

Figure 5 shows the waveform that represents solar irradiation. Due to intermittent nature of solar energy, it is seen that an initial energy output of 750 W/m^2 climbs to a value of 1000 W/m^2 after 0.1 s and then remains stable.

Table 1. Parameter specifications.

Parameters	Ratings
Solar panel	
Peak power	3 kW
No. of photovoltaic (PV) panels	250 W, 12 panels
Short circuit voltage V_{sc}	12 V
Open circuit voltage V_{oc}	22.6 V
Short circuit current I_{sc}	20.833 A
No. of series connected solar PV cells	36
Trans Z source based Luo converter	
Switching frequency f	10 kHz
Inductors L_1, L_2, L_3	4.7 mH
Capacitors C_1, C_2, C_3, C_4	22 µF
Output capacitor C_o	2200 µF
Brushless direct current (BLDC motor)	
Speed	3000 rpm
Load inertia	9×10^{-4} Nm^2

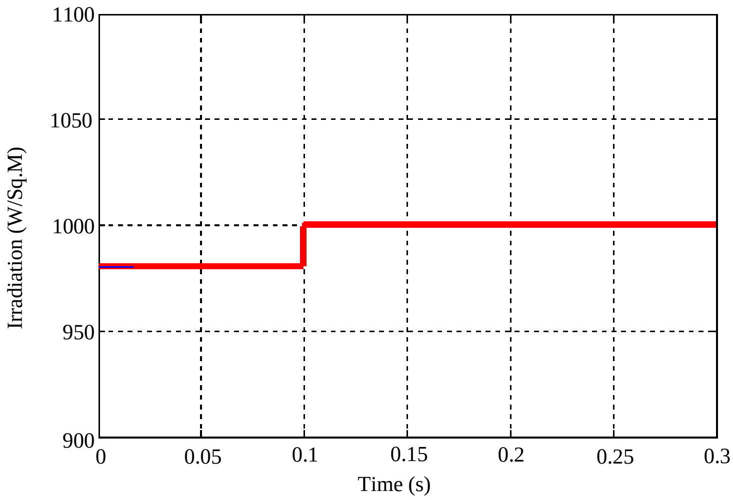

Figure 5. Solar irradiation waveform.

In Figure 6, the voltage produced by a solar panel is shown. Utilizing solar radiation, the solar panel collects energy and initially produces a voltage of 79 V. Due to observation of additional energy in the panel after 0.1 s, a voltage of 80 V is attained and kept constant after that.

The waveform shown in Figure 7 illustrates the output current achieved using a solar panel. It is observed that a minimal initial current of 17.3 A is maintained, and that after 0.1 s the current increases to 18.7 A and remains stable. In Figure 8, power obtained by a solar PV panel is shown as a waveform. The power is initially maintained at 1360 W for the first 0.1 s, after which it tends to increase and stay at 1500 W.

Improved converter output is the product of an efficient controller and controller strategies. The output voltage waveform produced by the suggested TZSBLC converter with the help of a PI controller is shown in Figure 9. The waveform shows that voltages vary initially, peaking at 330 V, then steadily decline before starting to fluctuate again. Later, at 0.26 s, the voltage stabilizes and is kept constant at 260 V.

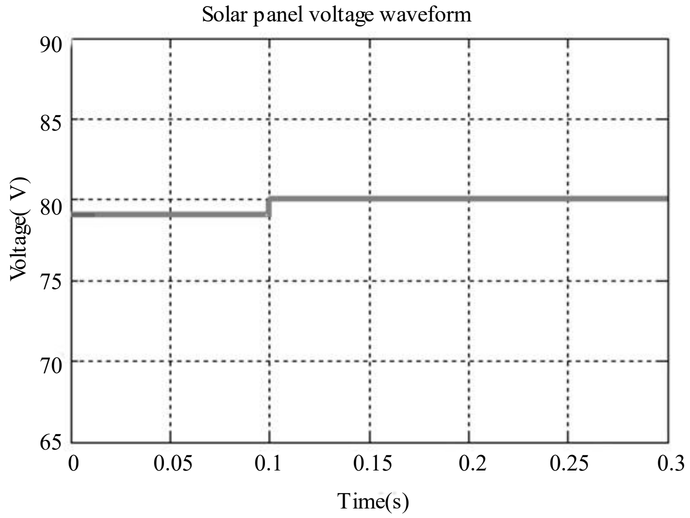

Figure 6. Photovoltaic (PV) voltage waveform.

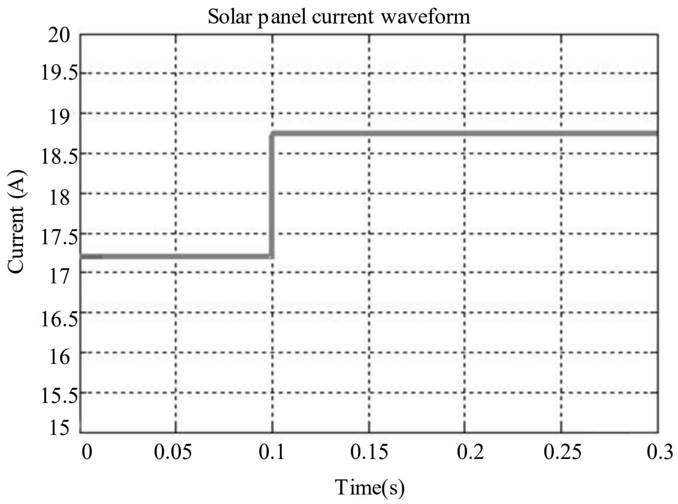

Figure 7. Photovoltaic (PV) current waveform.

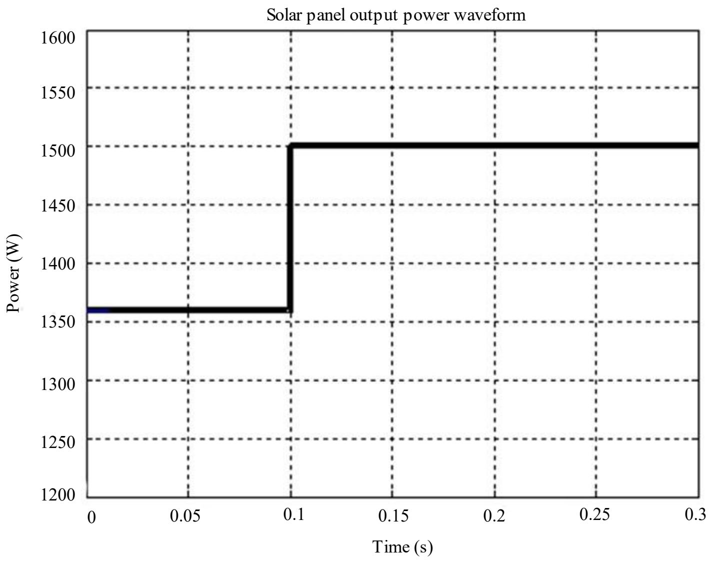

Figure 8. Photovoltaic (PV) power waveform.

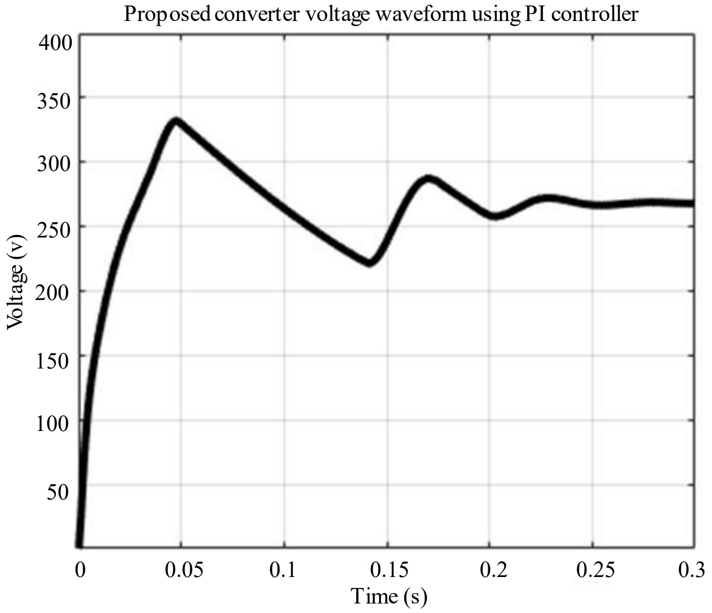

Figure 9. Voltage waveform using proportional integral (PI) controller.

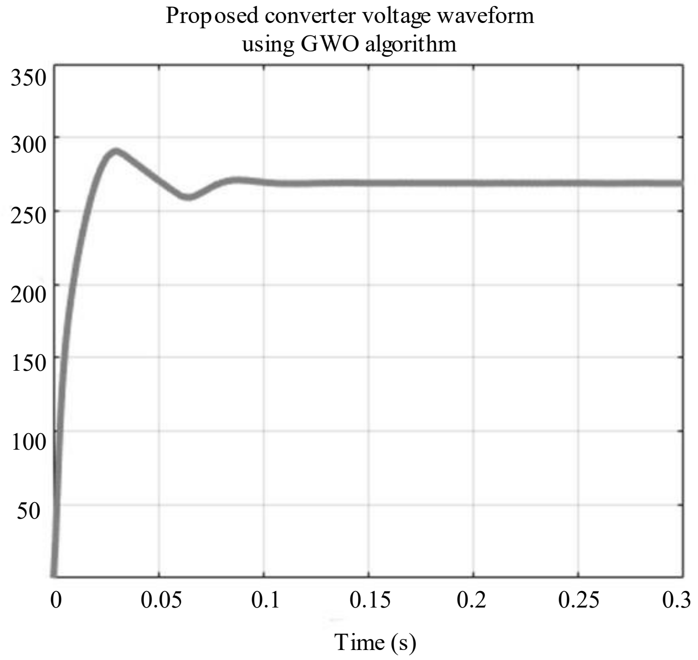

Figure 10. Voltage waveform using Grey Wolf optimized (GWO) algorithm.

Furthermore, the TZSBLC converter is managed using the GWO algorithm in order to improve the output voltage. At 0.05 s, the voltage reaches its maximum of 300 V and is thereafter steadily maintained. The voltage stabilizes at 0.17 s and tends to stay that way, as illustrated in Figure 10.

As shown in Figure 11, the developed TZSBLC converter is used in conjunction with a hybrid optimization strategy to produce a superior output voltage. A stable voltage of 260 V is attained after 0.15 s of initially moderate voltage rise and mild distortion, and it has the potential to last longer.

Figure 12 shows a waveform that represents single phase grid voltage. It has been noted that 230 V remains constant during both the half cycles.

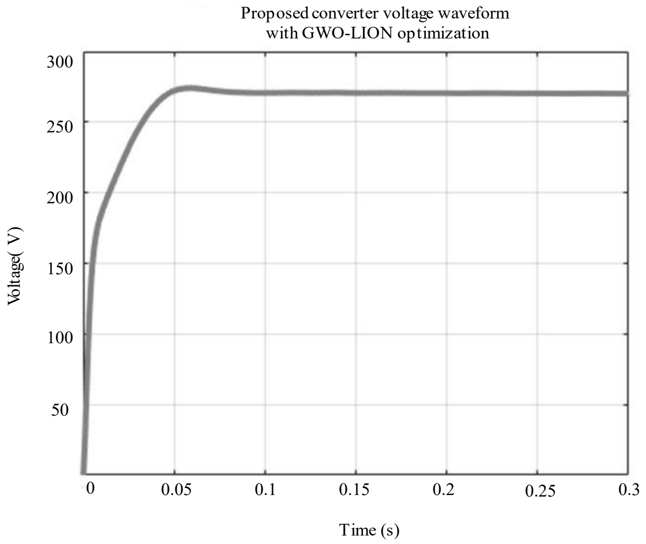

Figure 11. Voltage waveform using Grey Wolf optimization (GWO)–Lion optimization.

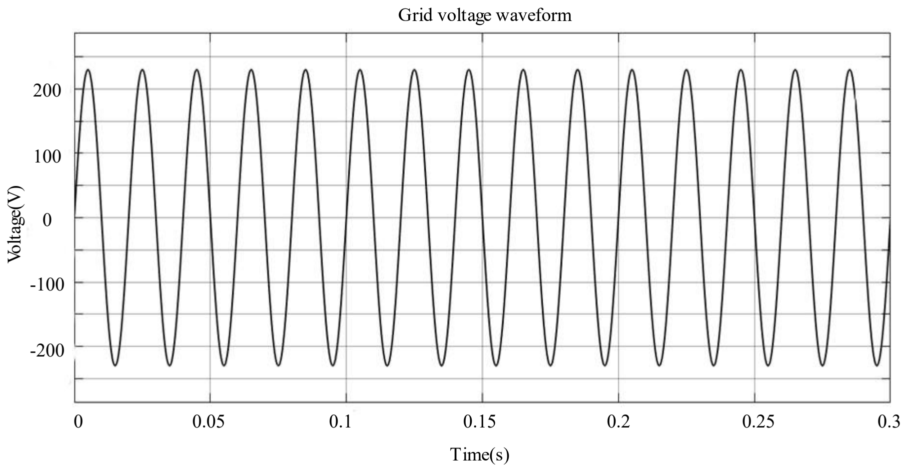

Figure 12. Grid voltage waveform.

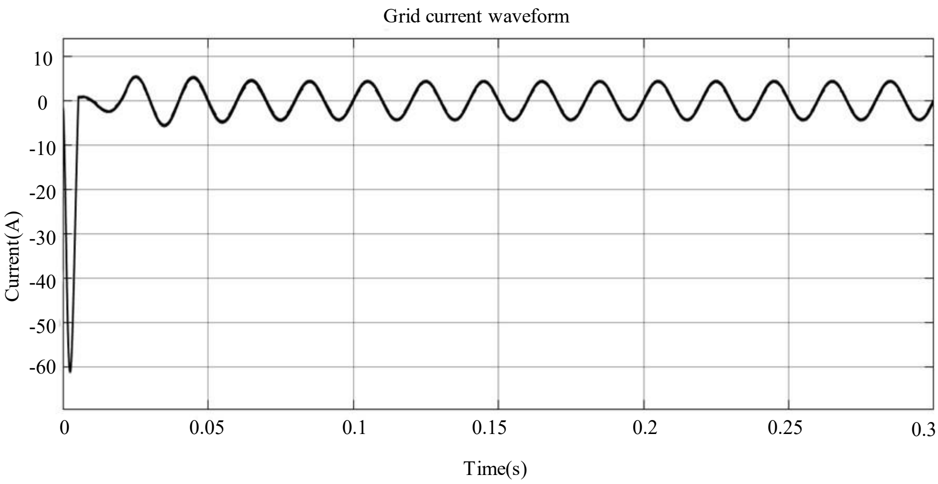

Figure 13. Grid current waveform.

Waveform illustrating grid current is demonstrated in Figure 13. It has been noted that a constant of 5 A is sustained after 0.03 s and tends to remain constant when current increases from the negative half cycle. Figure 14 displays the obtained waveform illustrative of real power. Real power is seen to climb from a negative value to a peak of 600 W before progressively declining. A 500 W actual power is kept stable and continues after 0.1 s.

Figure 15 shows the proof of reactive power produced by the suggested work. The power steadily decreases after reaching its peak of 1350 W and is maintained at its lowest level after 0.1 s without any aberrations.

Figure 16 depicts the waveform demonstrating of the current generated by BLDC motor. The current initially fluctuates higher before being kept at a low level with only a slight distortion. A continuous current of 5 A is kept constant and usually continues after 0.25 s.

The waveform illustrating BLDC motor back electromotive force (EMF) is shown in Figure 17. Back EMF is often a measurement of the voltage produced by a BLDC motor's rotor. This motor ignores the applied voltage and instead produces sinusoidal AC voltage, which is sustained at a constant 80 V after 0.03 s.

In Figure 18, the waveform that represents rotational velocity is depicted. It is seen that the speed progressively rises and then maintains itself at 2000 rpm after 0.05 s, giving the axis rotation speed for the number of full rotations.

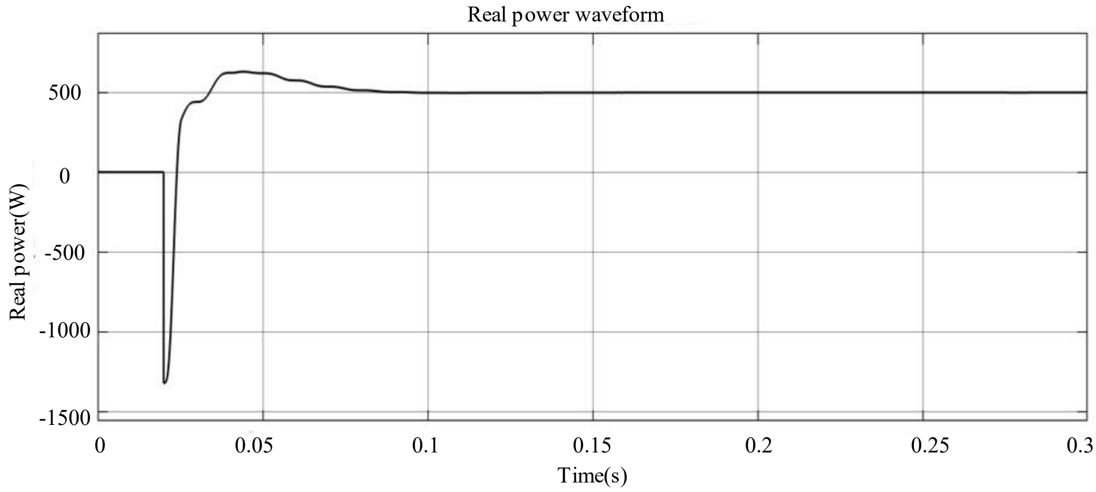

Figure 14. Actual power waveform.

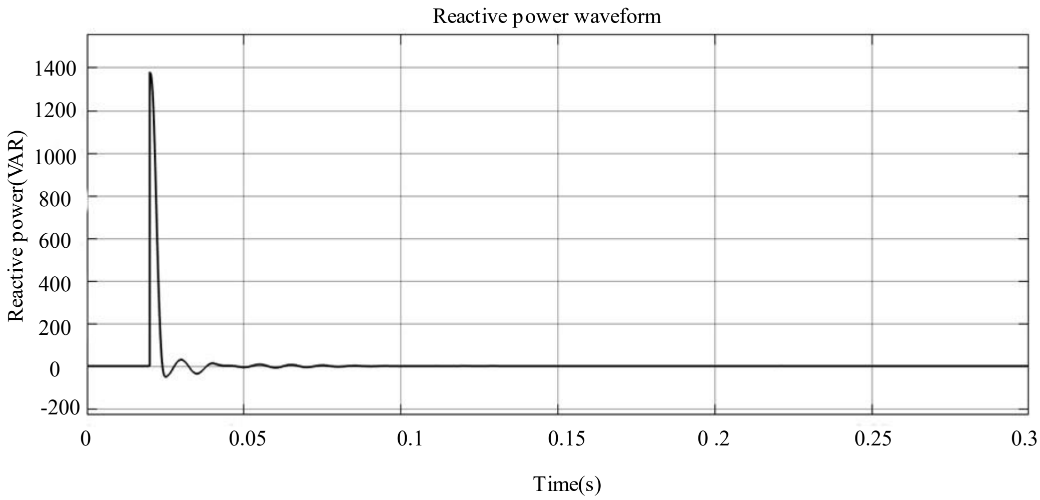

Figure 15. Reactive power waveform.

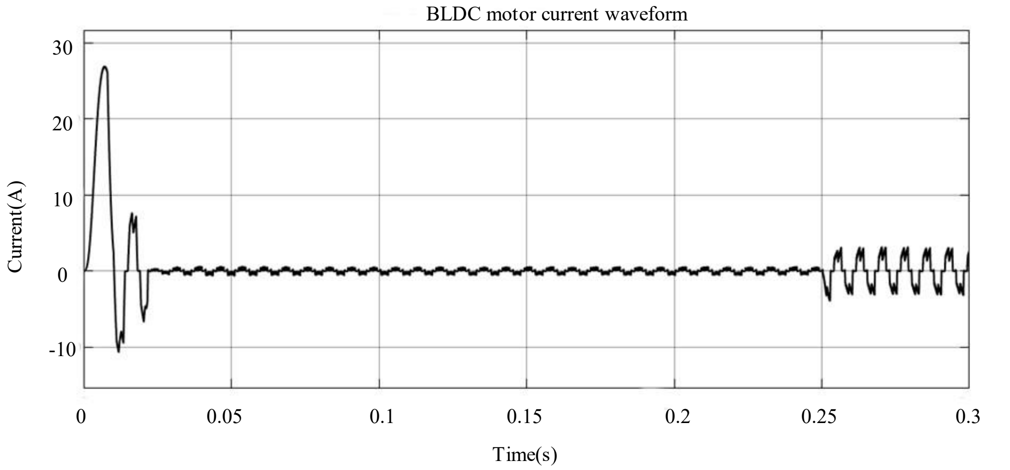

Figure 16. Motor current waveform.

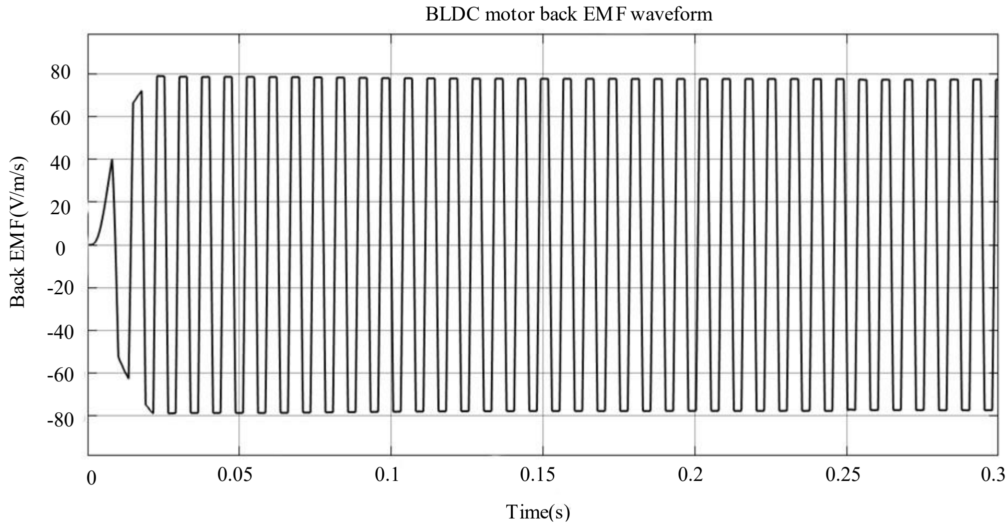

Figure 17. Back electromotive force (EMF) waveform of brushless direct current (BLDC) motor.

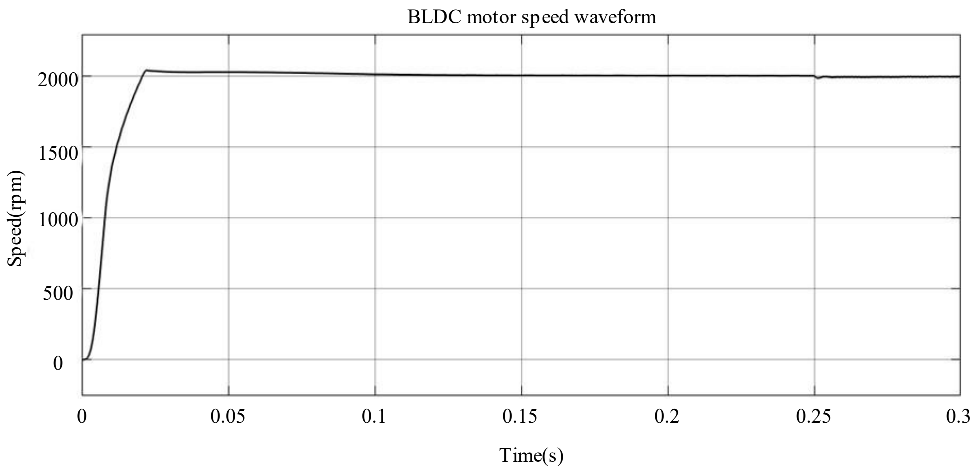

Figure 18. Speed waveform of brushless direct current (BLDC) motor.

In Figure 19, the waveform indicating the torque of a BLDC motor is shown. The torque is seen to be initially increasing and reaches a peak at 20 Nm at 0.02 s, then gradually drop. A minimum torque is achieved at 0.05 s with only slight distortion, and after0.24 s, it tends to rise to 3 Nm.

The harmonics obtained in suggested work is revealed in Figure 20. It has been noted that using a TZSBLC converter results in a reduced THD value that complies with IEEE standards at 4.43%.

Hardware Analysis

The FPGA Spartan 6E controller is used to implement the hardware analysis of proposed grid-tied solar EV charging system built with help from TZSBLC, and the results are then thoroughly examined. Figure 21 presents the hardware prototype in a clear and effective way. In Figure 22, the hardware findings for the PV's voltage and current output are shown. The output of the PV system increases as the temperature rises. Even with small fluctuations, the PV's output current is stable.

In Figure 23, the waveforms for TZSBLC's output voltage with and without optimization are shown. Without optimization, peak overshoot circumstances have an impact on the converter output, as shown in the figure, but with the use of an appropriate optimization technique, the peak overshoot condition problem is solved and a steady output of 330 V is attained.

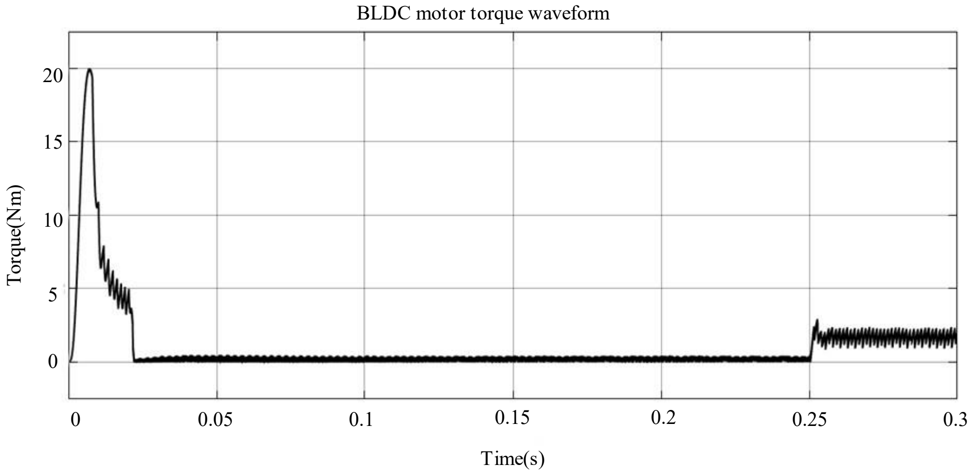

Figure 19. Torque waveform of brushless direct current (BLDC) motor.

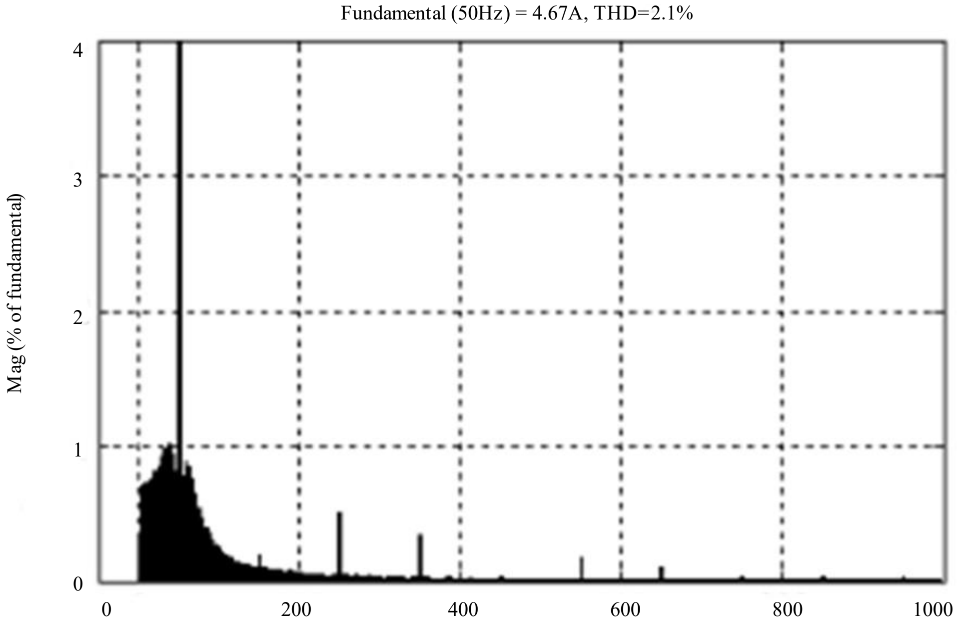

Figure 20. Total harmonic distortion (THD) waveform.

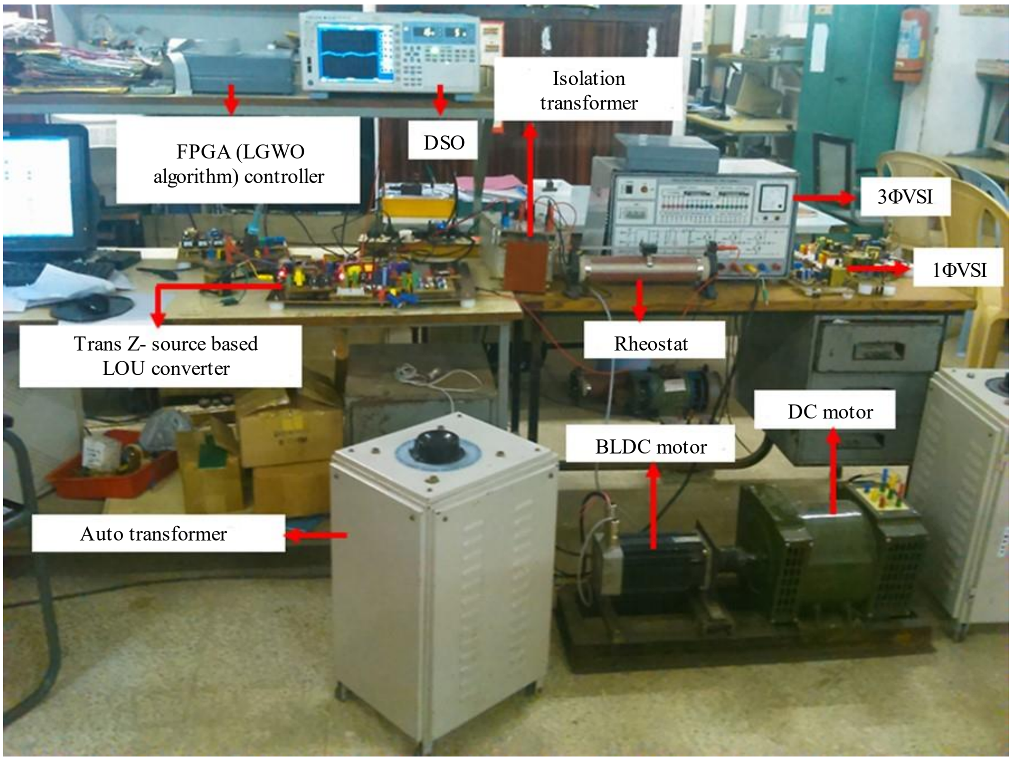

Figure 21. Hardware prototype setup.

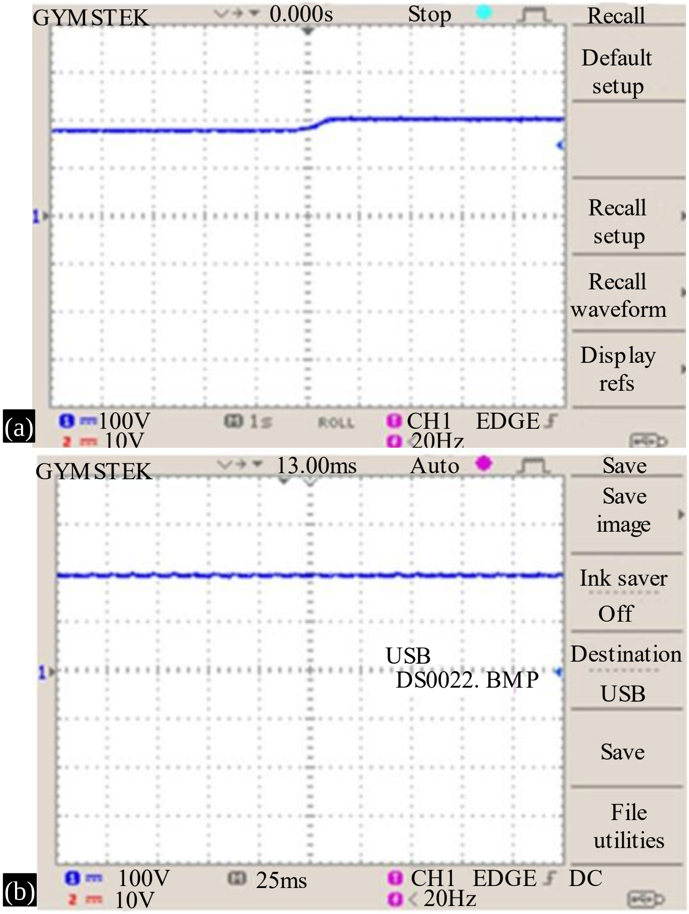

Figure 22. Photovoltaic system: (a) voltage and (b) current waveform.

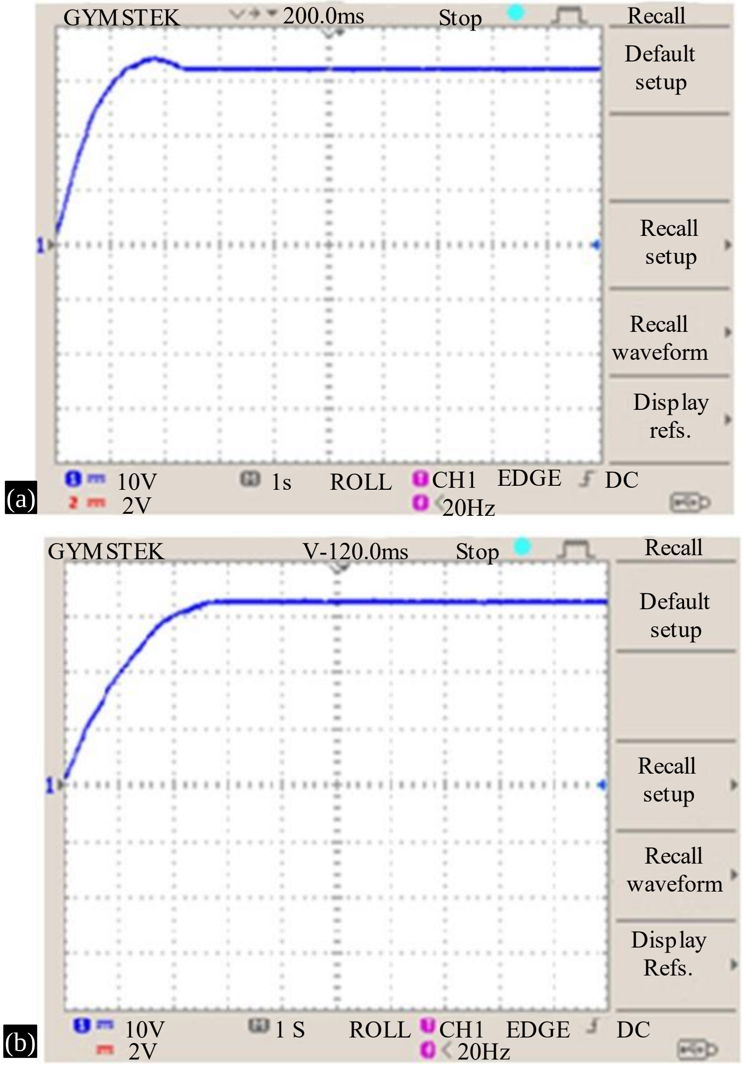

Figure 23. Converter output: (a) without optimization and (b) with optimization.

The reference speed of BLDC motor is set to 1500 rpm. After using suggested hybrid optimal controller, the speed is successfully controlled and remains stable, as shown in Figure 24(b). The actual and reference speeds are marked in blue and red, respectively. Without the use of an optimization controller, the BLDC motor's speed response characteristics are shown in Figure 24(a).

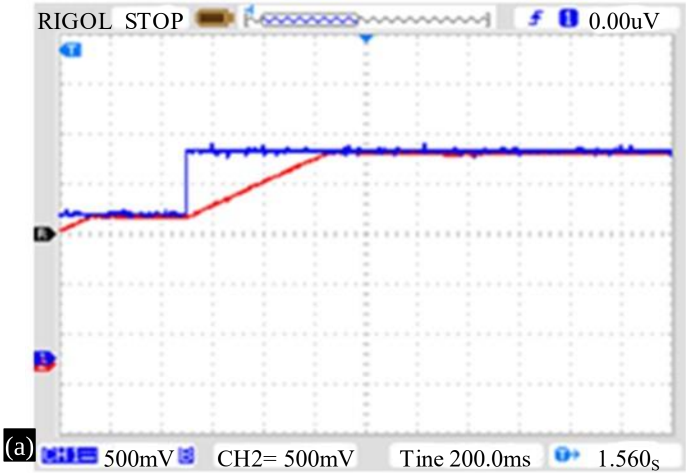

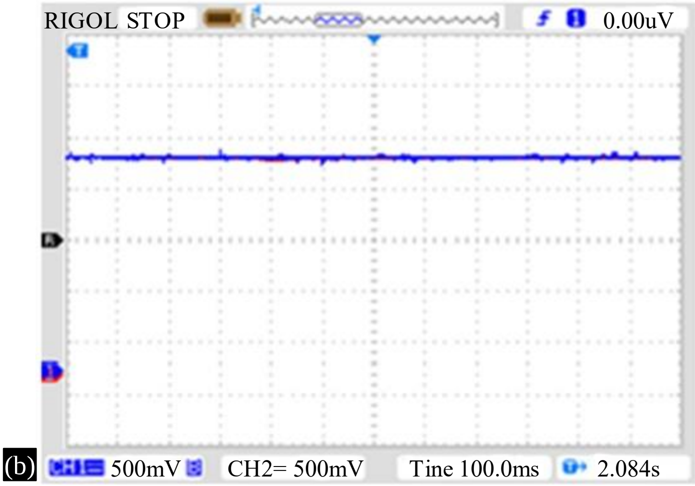

Figure 24. Speed waveform at 1500 rpm: (a) without optimization controller and (b) with optimization controller.

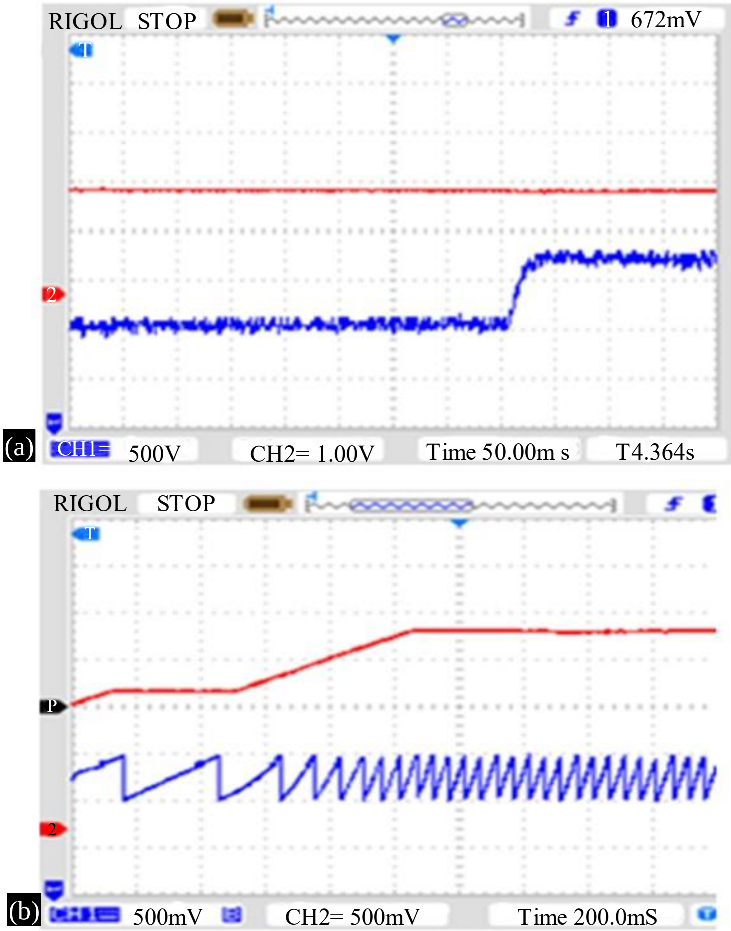

Figure 25. Brushless direct current (BLDC) motor: (a) speed and (b) torque waveform.

The suggested closed loop speed control technique shown in Figure 16 successfully regulates and stabilizes the speed and torque of the BLDC motor without experiencing peak overshoot problems.

Effective grid voltage synchronization is accomplished using PI controller, resulting in a consistent 230 V AC supply being provided to the grid from the inverter, as shown in Figure 26.

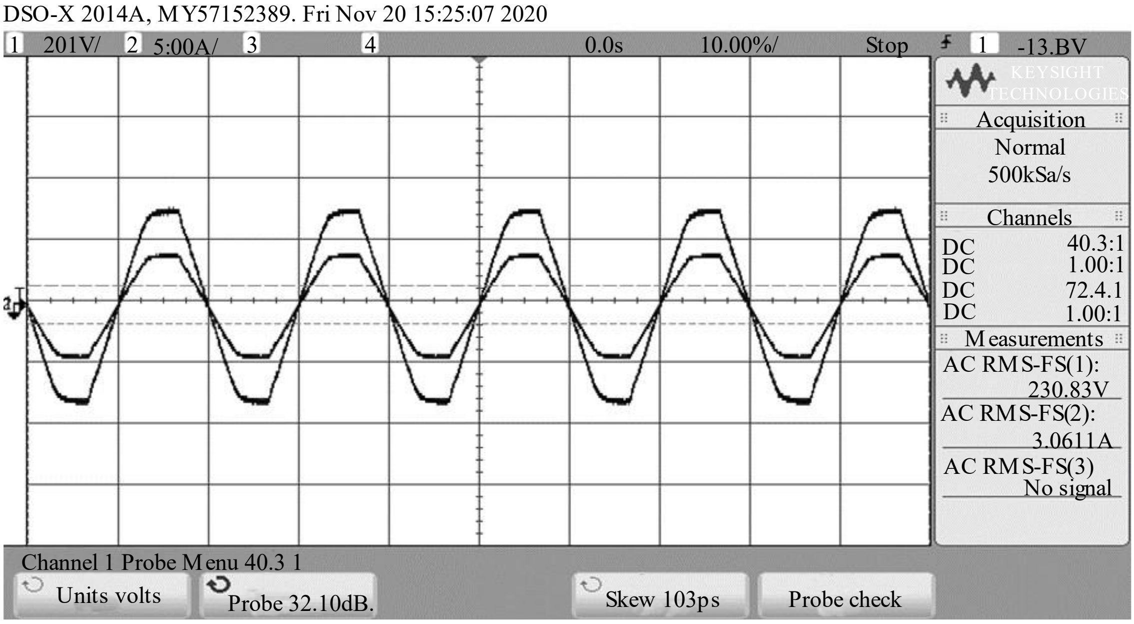

Figure 26. Grid voltage and current waveforms.

CONCLUSION

This paper presents a novel GWO-Lion optimization controller for considerably strengthening the performance of converter in order to reduce issues like THD, settling time, and peak overshoot. Subsequently, the waveform result obtained using MATLAB Simulink for the proposed converter and motor are described along with hardware outputs. Thus, utilizing this converter results solving the aforementioned issues and provides improved system performance. Using MATLAB simulation, the performance of the suggested PV-based BLDC motor using TZSBLC and LGWO-PI controller is evaluated, and the results are clearly analyzed. A comparative analysis is performed in terms of voltage gain, efficiency, THD and settling time for converters along with control approaches. By utilizing TZSBLC achieves an efficiency of 97.6%, voltage gain value of 1:16 and THD of 2.1% resulting in reduced harmonics with high system performance. Similarly, with the utilization of TZSBLC along with LGWO-PI controller provides remarkable performance in stabilizing voltage at a minimized settling time of 0.15 s is achieved by which the voltage settles earlier in contrast to the state-of-the-art method. The findings of this research conclude that the proposed system has advantageous like enhanced system performance, improved stability, reduced harmonics and high converter efficiency.

Funding Statement

The author received no specific funding for this study.

Conflicts of Interest

The author declares that he has no conflicts of interest to report regarding the present study.

REFERENCES

1. de Quevedo PM, Munoz-Delgado G, Contreras J. Impact of electric vehicles on the expansion planning of distribution systems considering renewable energy, storage, and charging stations. IEEE Trans Smart Grid. 2017; 10 (1): 794–804.
2. Yi P, Zhu T, Jiang B, Jin R, Wang B. Deploying energy routers in an energy internet based on electric vehicles. IEEE Trans Vehic Technol. 2016; 65 (6): 4714–4725.
3. Chen Q, Liu N, Hu C, Wang L, Zhang J. Autonomous energy management strategy for solid-state transformer to integrate PV-assisted EV charging station participating in ancillary service. IEEE Trans Indus Inform. 2016; 13 (1): 258–269.

4. Murali S, Panda KP, Panda G. PV-HESS fed BLDC driven water pumping system with PSO-based MPP tracking employing zeta converter. In: 2018 IEEE Innovative Smart Grid Technologies – Asia (ISGT Asia), Singapore, May 22–25, 2018. pp. 196–201.
5. Kumar R, Singh B. Single stage solar PV fed brushless DC motor driven water pump. IEEE J Emerg Select Top Power Electron. 2017; 5 (3): 1377–1385.
6. Kumar R, Singh B. Grid interactive solar PV-based water pumping using BLDC motor drive. IEEE Trans Indus Appl. 2019; 55 (5): 5153–5165.
7. Aliabadi SF, Taher SA, Shahidehpour M. Smart deregulated grid frequency control in presence of renewable energy resources by EVs charging control. IEEE Trans Smart Grid. 2016; 9 (2): 1073–1085.
8. Shanmugam SK, Ramachandran S, Arumugam S, Pandiyan S, Nayyar A, Hossain E. Design and implementation of improved three port converter and B4-inverter fed brushless direct current motor drive system for industrial applications. IEEE Access. 2020; 8: 149093–149112.
9. Zhou S, Zhou G, Zeng S, Xu S, Ma H. Unified discrete-mapping model and dynamical behavior analysis of current-mode controlled single-inductor dual-output DC–DC converter. IEEE J Emerg Select Top Power Electron. 2018; 7 (1): 366–380.
10. Du S, Wu B, Zargari NR. A transformer less high-voltage DC–DC converter for DC grid interconnection. IEEE Trans Power Delivery. 2017; 33 (1): 282–290.
11. Lee SH, Choi D, Park JW. Power-sensitivities-based indirect voltage control of renewable energy generators with power constraints. IEEE Access. 2021; 9: 101655–101664.
12. Kung SH, Kish GJ. A modular multilevel HVDC buck–boost converter derived from its switched-mode counterpart. IEEE Trans Power Delivery. 2017; 33 (1): 82–92.
13. Zhou S, Qiu Y, Zou F, He D, Yu P, Du J, Luo X, Wang C, Wu Z, Gu W. Dynamic EV charging pricing methodology for facilitating renewable energy with consideration of highway traffic flow. IEEE Access. 2019; 8: 13161–13178.
14. Granados-Luna TR, Araujo-Vargas I, Forsyth AJ, Cano-Pulido K, Velázquez-Elizondo PE, Cervantes I, Gómez-Olguín F, Villarruel-Parra A. Two-phase, dual interleaved buck–boost DC–DC converter for automotive applications. IEEE Trans Indus Appl. 2019; 56 (1): 390–402.
15. Tey KS, Mekhilef S, Seyedmahmoudian M, Horan B, Oo AT, Stojcevski A. Improved differential evolution-based MPPT algorithm using SEPIC for PV systems under partial shading conditions and load variation. IEEE Trans Indus Inform. 2018; 14 (10): 4322–4333.
16. Du W, Zhong W, Tang Y, Du W, Jin Y. High-dimensional robust multi-objective optimization for order scheduling: a decision variable classification approach. IEEE Trans Indus Inform. 2018; 15 (1): 293–304.
17. Wang W, Zhao J, Zhou Y, Dong F. New optimization design method for a double secondary linear motor based on R-DNN modeling method and MCS optimization algorithm. Chinese J Electric Eng. 2020; 6 (3): 98–105.
18. Long W, Jiao J, Liang X, Cai S, Xu M. A random opposition-based learning Grey Wolf optimizer. IEEE Access. 2019; 7: 113810–113825.
19. Chen X, Zhang T, Ye W, Wang Z, Iu HH. Blockchain-based electric vehicle incentive system for renewable energy consumption. IEEE Trans Circuits Systems II Express Briefs. 2020; 68 (1): 396–400.
20. Zheng Y, Ho M, Guo J, Leung KN. A single-inductor multiple-output auto-buck–boost DC–DC converter with tail-current control. IEEE Trans Power Electron. 2015; 31 (11): 7857–7875.
21. Sun Y, Yue H, Zhang J, Booth C. Minimization of residential energy cost considering energy storage system and EV with driving usage probabilities. IEEE Trans Sustain Energy. 2018; 10 (4): 1752–1763.
22. Huang Y, Xu Y, Li Y, Yang G, Zou J. PWM frequency voltage noise cancelation in three-phase VSI using the novel SVPWM strategy. IEEE Trans Power Electron. 2017; 33 (10): 8596–8606.
23. Cheng YF, Shao W, Zhang SJ, Li YP. An improved multi-objective genetic algorithm for large planar array thinning. IEEE Trans Magnet. 2015; 52 (3): 1–4.

24. Cho YK, Lee KC. Noninverting buck–boost DC–DC converter using a duobinary-encoded single-bit delta-sigma modulator. IEEE Transac Power Electron. 2019; 35 (1): 484–495.
25. Liang Y, Zhang H, Du M, Sun K. Parallel coordination control of multi-port DC-DC converter for stand-alone photovoltaic-energy storage systems. CPSS Trans Power Electron Appl. 2020; 5 (3): 235–241.
26. Li Z, Tam V, Yeung LK. An adaptive multi-population optimization algorithm for global continuous optimization. IEEE Access. 2021; 9: 19960–19989.

